

RSC Advances



This is an *Accepted Manuscript*, which has been through the Royal Society of Chemistry peer review process and has been accepted for publication.

Accepted Manuscripts are published online shortly after acceptance, before technical editing, formatting and proof reading. Using this free service, authors can make their results available to the community, in citable form, before we publish the edited article. This *Accepted Manuscript* will be replaced by the edited, formatted and paginated article as soon as this is available.

You can find more information about *Accepted Manuscripts* in the [Information for Authors](#).

Please note that technical editing may introduce minor changes to the text and/or graphics, which may alter content. The journal's standard [Terms & Conditions](#) and the [Ethical guidelines](#) still apply. In no event shall the Royal Society of Chemistry be held responsible for any errors or omissions in this *Accepted Manuscript* or any consequences arising from the use of any information it contains.

ARTICLE

Cite this: DOI:
10.1039/x0xx00000x

Received 00th January 2012,
Accepted 00th January 2012

DOI: 10.1039/x0xx00000x

www.rsc.org/

Hybrid Nanoporous Polystyrene Derived from Cubic Octavinylsilsesquioxane and Commercial Polystyrene *via* the Friedel-Crafts Reaction

Yue Wu,^{a,b} Ligu Li,^b Wenyan Yang,^b Shengyu Feng^b and Hongzhi Liu^{*a,c}

A series of hybrid nanoporous polystyrenes were synthesized from commercial polystyrene (PS) and cubic octavinylsilsesquioxane (OVS) *via* the Friedel-Crafts reaction. The porosity of the resulting hybrid polymers could be fine-tuned by varying the ratio of PS and OVS. The resulting polymers, HCP-1 to HCP-9 with the apparent Brunauer–Emmett–Teller surface areas (S_{BET}) were in a range of 2.6 to 767 $\text{m}^2 \text{g}^{-1}$, with total pore volumes in the range of 0.36 to 0.90 $\text{cm}^3 \text{g}^{-1}$. The S_{BET} was maximum when OVS loading was 9.1 wt %; it then decreased till almost no porosity before increasing again with the increase of OVS loading. The thermal decomposition temperatures of the hybrid polymers were close to pure PS under N_2 atmosphere, but the residues increased with the increase of OVS loading. The gas sorption applications revealed that HCP-3 possessed H_2 uptake of 3.01 mmol g^{-1} (0.60 wt %) at 77 K and 1.01 bar and CO_2 uptake of 1.12 mmol g^{-1} (4.93 wt %) at 298 K and 1.01 bar.

Introduction

Porous materials with novel intrinsic properties such as high specific surface area, excellent porosity and good thermal stability have potential applications in gas storage and separation,^[1] optical devices,^[2,3] heterogeneous catalysis,^[4,5] etc. Covalently-linked porous polymers have attracted specific interest because their structures and properties are easily tuned through rational design.^[6] Polystyrene is a general polymer that has been widely used. It possesses well-known properties, such as ease of processing and functionalization, solubility in a broad range of solvents, outstanding thermal stability, and mild substrate as supporter.^[7] As the first organic porous resin to be industrialized, hypercrosslinking polystyrene was prepared by the Davankov^[8] using the linear polystyrene, divinylbenzene and the lightly crosslinked gel-type styrene-divinylbenzene (St-DVB) copolymers as the raw materials, postfunctionalized with the highly cross-linking and porous structures *via* the Friedel-Crafts reaction. The hypercrosslinking polystyrene had been widely used as the sorbents adsorbing the organic solvents^[9, 10], inorganic ions^[11, 12] and the gas^[13-15], and also used as the stationary phase in the column to separate the various materials^[16] due to its high porosities, lower density and excellent swelling properties. In addition, it had been used to prepare nanocomposites that exhibited excellent catalytic performance^[17, 18] and magnetic properties.^[19]

Research on inorganic-organic hybrid nanocomposites has grown rapidly because of their advantages of the combination of flexibility, processability of organic polymers with the rigidity and thermal stability of the inorganic component.^[20-22] Physically blending, interfacial interaction, in situ

polymerization and other methods are used to prepare these hybrid nanocomposites, which exhibit excellent thermal and mechanical properties. Silica nanoparticles have exhibited a good thermal, chemical stability with well-defined, size-tunable structure. Thus grafting different functional organic layers onto the silica particles has been explored in many areas.^[23-25] As a silica-like cage compound, polyhedral oligomeric silsesquioxane (POSS) provides an excellent platform for synthesis of new inorganic-organic hybrid materials with enhanced thermal and mechanical properties.^[26] POSS has been incorporated into polystyrene *via* chemical grafting, including ATRP, RAFT, anion polymerization, Friedel-Crafts reaction etc., to form hybrid polystyrenes of various molecular architectures. These hybrid polystyrene based on POSS exhibited the improved thermal stabilities,^[27,28] viscoelastic properties,^[29,30] magnetic properties^[31] compared to the pristine polystyrene. In addition, nonreactive octaphenethyl POSS was also used to prepare hybrid nanocomposites with PS *via* physical blending. Results showed that the octaphenethyl POSS could be incorporated into polystyrene up to 40 wt % without phase separation.^[32]

The “*bottom-up*” topology combination has proved to be an efficient strategy to construct porous materials.^[6,33] Rational selection of suitable rigid building blocks with different geometry will help to construct polymer networks with novel topology structures and properties. Linking the monomers with different geometries together can combine their advantages; in addition, the porosity and functionality of the resulting polymers could be easily tuned.^[34,35] Rigid cage make POSS become an ideal building block to construct novel inorganic-organic hybrid porous materials. Some hybrid porous materials

based on POSS have been synthesized by the reaction of other building blocks with different geometries.^[36,37]

Starting from cubic octavinylsilsequioxane (OVS), we have successfully prepared some hybrid porous materials by the combination with planar benzene or tetrahedral tetraphenylsilane (TPS) *via* the Friedel–Crafts reaction and tuned their porosities *by* adjusting the ratio of OVS to benzene or TPS utilizing the multi-reaction sites of aromatic groups.^[38,39] It was observed that S_{BET} increased with the increasing reactive sites of benzene, *i.e.* decreasing the ratio of benzene to OVS; however, the pore size distributions (PSDs) were wide and irregular and the pores changed from coexistent micro-mesopores to almost mesopores. The tunable porosity was correlated with the multi-reaction sites of benzene and thus diverse local cross-linking density in the networks formed by the Friedel–Crafts alkylation reaction.^[38] Consistent with this report, when TPS was used as a crosslinker, S_{BET} was also monotonously enhanced with decreasing the ratio of TPS because of the increasing crosslinking density, which could lead to higher surface areas up to $989 \text{ m}^2 \text{ g}^{-1}$. In comparison to benzene, TPS possessed a larger molecular volume and consisted of four phenyl groups, which could provide more connecting sites, acting as a concentrative crosslinker. Different from benzene as a crosslinker, the resulted porous materials exhibited uniform PSDs, *i.e.* micropores with an average diameter centered at about 1.5 nm and uniform mesopores with an average diameter centered at about 3.6 nm, which should be ascribed to the steric hindrance effect of TPS, making it more difficult to adjust its position during the reaction relative to benzene.^[39]

Covalently-linked porous polymers have been investigated widely, however most porous polymers arose from small building blocks.^[6] Using commercially available polymers as rigid building blocks to construct porous materials *via* simple modification is less reported by far. Owing to large rigid phenyl groups in polystyrene, it is possible to prepare hybrid porous polystyrenes through the topology combination with cubic OVS. Different from small aromatic molecules like benzene or TPS, it was expected that some novel porous materials could originate from the combination of polystyrene and OVS. More importantly, simple process and cheaper starting materials provide the possibility to economically prepare these porous materials in a large scale and make it possible to be industrialized.

In this paper, we attempt to use OVS to react with commercial linear polystyrene to prepare hybrid porous polymers *via* the Friedel–Crafts reaction. Their properties such as thermal properties, gas absorption and storage are also investigated. The resulting hybrid porous polymers exhibit high thermal stability, high porosity and high gas uptake ability in H_2 and CO_2 .

To our knowledge, this is the first report on the preparation of porous materials from commercial polymer and POSS. The successful preparation of hybrid porous materials from commercial polystyrene and cubic OVS will stimulate more works on porous materials from other commercial polymers and POSS.

Experimental.

Materials

The PS ($M_n = 2.6 \times 10^5$) was obtained from Aladdin-reagent limited Co., and used without further purification. OVS was

prepared according to previous reports.^[40] CS_2 was supplied by China National Medicines Group and purified using atmospheric distillation methods and stored with 4 Å molecule sieves prior to use.

Characterization

Fourier-transformed infrared (FT-IR) spectra were carried out using Bruker TENSOR27 infrared spectrophotometer from 400 to 4000 cm^{-1} at a resolution of 4 cm^{-1} . The samples were prepared using conventional KBr disk method. Solid-state ^{13}C CP/MAS NMR and ^{29}Si MAS NMR spectra were performed on Bruker AVANCE-500 NMR spectrometer operating at a magnetic field strength of 9.4 T. The resonance frequencies at this field strength were 125 and 99 MHz for ^{13}C NMR and ^{29}Si NMR, respectively. A chemagnetics of 5 mm triple-resonance MAS probe was used to acquire ^{13}C and ^{29}Si NMR spectra. ^{29}Si MAS NMR spectra with high power proton decoupling were recorded with $\pi/2$ pulse length of 5 μs , recycle delay of 120 s, and spinning rate of 5 kHz. Elemental analyses were conducted using Elementar vario EL III elemental analyzer.

Field-emission scanning electron microscopy (FE-SEM) experiments were characterized by a HITACHI S4800 spectrometer. Samples were dispersed in EtOH with the aid of sonication and a drop of ethanol suspension was loaded onto a carbon-coated copper grid and left to dry under infrared lamp; and the samples were coated by sputtering with a thin layer of Au prior to imaging. High-resolution transmission electron microscopy (HRTEM) experiments were recorded using a JEM 2100 electron microscope (JEOL, Japan) with an acceleration voltage of 200 kV. Samples were dispersed in EtOH with the aid of sonication, and a drop of ethanol suspension was loaded on the carbon-coated copper grid and was dried under the infrared lamp.

Thermal gravimetric analysis (TGA) was performed on a Mettler Toledo model SDTA 854 TGA system under N_2 atmosphere at a heating rate of $10 \text{ }^\circ\text{C min}^{-1}$ from room temperature to $800 \text{ }^\circ\text{C}$. Powder X-ray diffraction (PXRD) images were collected on a Rigaku D/MAX 2550 diffractometer under $\text{Cu-K}\alpha$ radiation, 40 kV, and 200 mA with a scanning rate of $10^\circ \text{ min}^{-1}$.

N_2 sorption isotherm measurements were characterized by a Micro Meritics surface area and pore size analyzer. Before measurement, the samples were degassed for 12 h at $160 \text{ }^\circ\text{C}$. A sample of ca. 100 mg and a UHP-grade N_2 (99.999%) gas source were adopted in the N_2 sorption measurements at 77 K and collected on a Quantachrome Quadrasorb apparatus. S_{BET} was confirmed over a P/P_0 range from 0.01 to 0.20. Nonlocal density functional theory (NL-DFT) pore size distributions (PSDs) were determined by C/slit-cylindrical pore mode of the Quadrawin software. CO_2 isotherms were measured at 298 K at 0.0 to 1.01 bar. H_2 adsorption capacity was measured at 77 K at 0.0 to 1.01 bar. Before measurement, the samples were degassed at $150 \text{ }^\circ\text{C}$ under vacuum for about 15 h.

Preparation of the hybrid polymers (HCPs)

Ar charged with polystyrene (1.00 g, $3.85 \times 10^{-2} \text{ mmol}$), catalytic amount of anhydrous AlCl_3 , stoichiometric OVS (Table 1) and CS_2 (10 mL) were placed in an oven-dried flask. The resulting mixture was vigorously stirred at room temperature for 0.5 h and under reflux for 24 h. Then the mixture was cooled to room temperature. For HCP-1 to HCP-2, the mixture was precipitated in ethanol and dried in vacuo at $60 \text{ }^\circ\text{C}$ for 48 h. For HCP-3 to HCP-9, the mixture was filtered and washed with ethanol, acetone, water, and tetrahydrofuran. The

slightly pink products were obtained under the Soxhlet extractor with dichloromethane for 48 h, and dried in vacuo at 60 °C for 48 h.

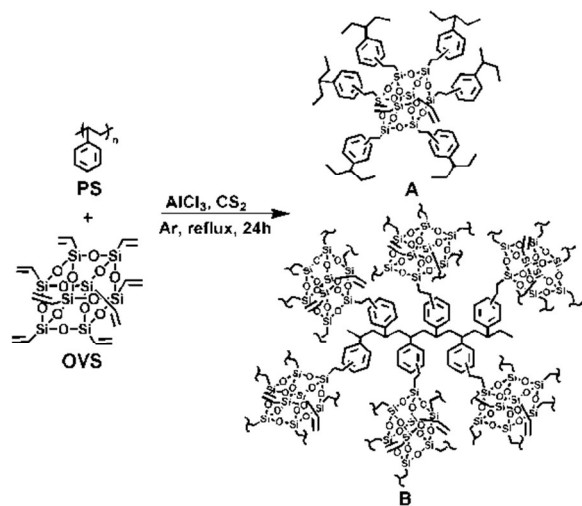
Table 1. Composition of the starting materials for HCP-1 to HCP-9

Sample	PS (mmol)	OVS (mmol)	OVS (wt %)	$M_{\text{vinyl}}/M_{\text{Phenyl}}^a$
HCP-1	3.85×10^{-2}	6.32×10^{-2}	3.8	0.052
HCP-2	3.85×10^{-2}	1.26×10^{-1}	7.4	0.10
HCP-3	3.85×10^{-2}	1.58×10^{-1}	9.1	0.13
HCP-4	3.85×10^{-2}	3.16×10^{-1}	16.7	0.26
HCP-5	3.85×10^{-2}	4.74×10^{-1}	23.1	0.39
HCP-6	3.85×10^{-2}	6.32×10^{-1}	28.6	0.53
HCP-7	3.85×10^{-2}	9.48×10^{-1}	37.5	0.79
HCP-8	3.85×10^{-2}	12.64×10^{-1}	44.4	1.1
HCP-9	3.85×10^{-2}	15.8×10^{-1}	50.0	1.3

^a The molar ratio of the Vinyl groups to the Phenyl groups.

Results and Discussion

As shown in Scheme 1, hybrid porous polymers were synthesized through the Friedel–Crafts reaction of OVS with stoichiometric PS in CS₂ under reflux for 24 h. For HCP-1 and HCP-2, they still dissolved in CS₂ and other solvents, for example, tetrahydrofuran, dichloromethane. For HCP-3 to HCP-9, the products were highly crosslinked and did not dissolve in CS₂ and other solvents. The content of carbon and hydrogen of HCPs was confirmed by elemental analysis, and the results were provided in the supporting information (S1).



Scheme 1. Synthetic routes for HCPs, and possible fragments A and B.

These hybrid polymers were first characterized by FT-IR spectra and the spectra of HCP-3, HCP-4 and HCP-8, HCP-9 were shown in Figure 1. The spectra of HCP-1, HCP-2, HCP-5, HCP-6 and HCP-7 were supported in the supporting information (S2 to S6). Compared with the FT-IR pattern of OVS, the intensities of the peaks at 1603 and 1410 cm⁻¹ decreased, which was associated with vinyl groups^[41] of HCP-3 to HCP-9, indicating that the polymerization reaction occurred. The peaks between 3080 and 2843 cm⁻¹ could be assigned to C-

H stretching vibration of aromatic, vinyl, methyl and methylene groups. The strong peak at ~1113 cm⁻¹ was attributed to typical Si-O-Si stretching vibrations, and the results proved that cubic silsesquioxane cages existed in these hybrid porous materials.^[42-44]

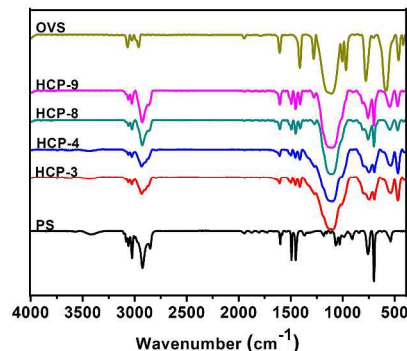


Figure 1. FT-IR of the OVS, PS, HCP-3, HCP-4 and HCP-8, HCP-9

The chemical structures of these hybrid polymers were also determined by the solid-state ¹³C CP/MAS NMR and ²⁹Si MAS NMR spectroscopy. Owing to their similar solid ¹³C CP/MAS NMR and ²⁹Si MAS NMR spectra for these hybrid polymers, HCP-3 was selected as a representative example to analyze. The solid-state ¹³C CP/MAS NMR spectrum of HCP-3 was displayed in Figure 2(a). The resonance peaks in the range of 128 to 142.6 ppm were

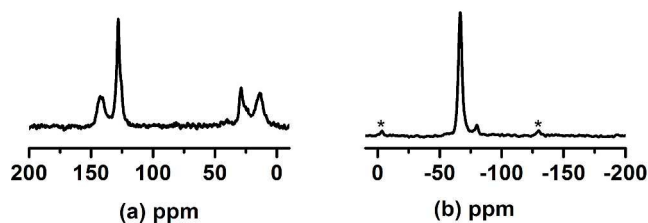


Figure 2. (a) Solid-state ¹³C MAS NMR spectrum of HCP-3. (b) Solid-state ²⁹Si MAS NMR spectrum of HCP-3.

ascribed to the carbon atoms derived from the bridging aromatic units and the unreacted Si-CH=CH₂. The resonance peak at the 28.8 ppm was attributed to the β C atoms at the linker units of -Si-CH₂-CH₂- formed after the Friedel–Crafts reaction. The resonance peak at the 13.8 ppm was attributed to the α C atoms at the linker units of -Si-CH₂-CH₂- formed after the Friedel–Crafts reaction and thus results further confirmed the success of the cross-linking reaction. The solid-state ²⁹Si MAS NMR spectrum of the HCP-3 (Figure 2(b)) showed that the resonance peaks at the -67 and -80 ppm could be ascribed to the silicon atoms of T₃ units (T_n: CSi(OSi)_n(OH)_{3-n}) from the Si-CH₂-CH₂- units formed after the Friedel–Crafts reaction and the unreacted Si-CH=CH₂ units, respectively. Compared with other POSS-based porous polymers,^[37,44] no T₁ or T₂ unit was observed, suggesting that no POSS cage collapsed in the frameworks during synthesis, which was consistent with our previous report.^[38] The two peaks at ~-5 ppm and ~-130 ppm were two reference peaks.

The porous structure of HCPs was investigated by N₂ adsorption-desorption analysis at 77 K. The N₂ isotherms showed that HCP-1, HCP-2, HCP-5, HCP-6 and HCP-7 had the nominal surface area of 2.6, 2.6, 38, 12 and 41 m² g⁻¹, respectively. The results indicated that there was almost no pore

in these hybrid polymers. The other N_2 isotherms of HCP-3, HCP-4, HCP-8 and HCP-9 were shown in the Figure 3. Four

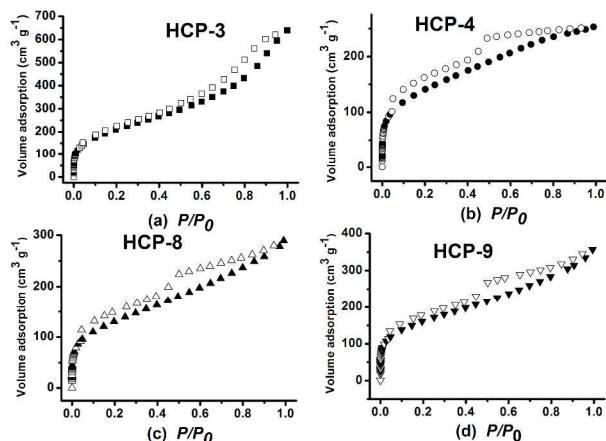


Figure 3. N_2 sorption isotherms of the HCP-3, HCP-4, HCP-8 and HCP-9

hybrid polymers exhibited a combination of type I and type IV N_2 gas sorption isotherms according to IUPAC classifications and were consistent with the previous reports. The isotherms of HCP-3, HCP-4, HCP-8 and HCP-9 show a steep nitrogen gas uptake at low relative pressure ($P/P_0 < 0.001$), reflecting that there existed some amounts of micropores in the networks structure, and there is gradually increasing gas uptake at higher relative pressures ($P/P_0 > 0.5$) with a clear hysteresis, indicating that these materials contained mesopores.^[45] Besides, the gas uptake isotherm of HCP-3 was slightly steeper than other three isotherms at higher relative pressures, which suggested that the contribution of mesopores in the HCP-3 was higher than the HCP-4, HCP-8 and HCP-9. The detailed porosity data of these polymers were shown in Table 2. The apparent BET specific surface areas (S_{BET}) of HCP-3, HCP-4, HCP-8 and HCP-9 were 767, 509, 473, and 582 $m^2 g^{-1}$, respectively. The total pore volumes (V_{TOTAL}) of the networks were 0.90, 0.36, 0.40 and 0.49 $cm^3 g^{-1}$ calculated at $P/P_0 = 0.99$, respectively. The S_{BET} of hybrid polymers firstly increased up to a maximum value, subsequently decreased before increasing with the increase of OVS loading. S_{BET} of hybrid polymer was maximum when OVS loading was 9.1 wt %; when OVS loading was 3.8, 7.4, 23.1, 28.6, 37.5 wt %, respectively, there was no porosity for HCP-1, HCP-2, HCP-5, HCP-6 and HCP-7.

Table 1. Porosity data of HCP-1 to HCP-9

Sample	$S_{BET}^{[a]}/$ $m^2 g^{-1}$	$S_{micro}^{[b]}/$ $m^2 g^{-1}$	$V_{total}^{[c]}/$ $cm^3 g^{-1}$	$V_{micro}^{[d]}/$	V_{micro}/V_{total}
HCP-1	2.6				
HCP-2	2.6				
HCP-3	767	154	0.90	0.06	0.07
HCP-4	509	169	0.36	0.08	0.22
HCP-5	38				
HCP-6	12				
HCP-7	41				
HCP-8	473	128	0.40	0.06	0.15

HCP-9	582	208	0.49	0.09	0.18
-------	-----	-----	------	------	------

(a) Surface area calculated from N_2 adsorption isotherm using BET method. (b) Microporous surface area calculated from N_2 adsorption isotherm using t-plot method. (c) Total pore volume calculated at $P/P_0 = 0.99$. (d) Micropore volume derived using t-plot method based on the Halsey thickness equation.

The pore size distributions (PSDs) of these hybrid hypercrosslinking polystyrenes were calculated by nonlocal density functional theory (NL-DFT), and the results were displayed in Figure 4. HCP-3 possessed relatively uniform micropores with an average diameter centered at 1.4 nm and a broader distribution of mesopores from 2.2 to 14.5 nm. HCP-4, HCP-8 and HCP-9 also displayed uniform micropores with an average diameter centered at 1.4 nm and a narrower distribution of mesopores from 2.2 nm to 4.4 nm compared with HCP-3. The PSD results were consistent with the shape of N_2 isotherms, indicating that micropores and mesopores coexisted in the hybrid polymers.

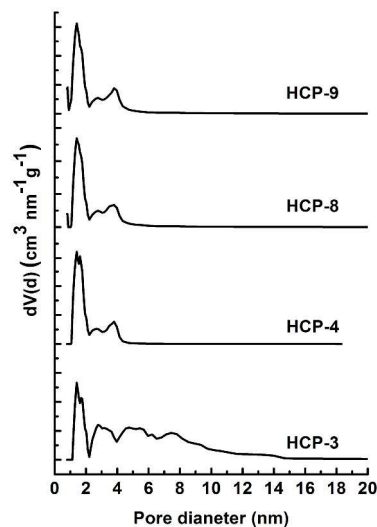


Figure 4. NL-DFT PSDs of the HCP-3, HCP-4, HCP-8 and HCP-9

There are several factors to explain the variation in the surface area and pores size distribution of these hybrid polymers. According to the previous reports, traditional hypercrosslinking porous polystyrenes were prepared by the precursor of linear polystyrene through adding small molecule of divinyl benzene as a crosslinking agent *via* the Friedel-Crafts alkylation reaction.^[46] During the process, initial polystyrene coils, a cross-agent and a Friedel-Crafts catalyst were homogeneously distributed throughout the whole volume of their solution in ethylene dichloride. The polymeric chains extended through the whole initial solution (or gel) and remained strongly solvated over all period of network formation. Intra- and intermolecular cross-linking simultaneously emerged throughout the entire volume of the reacting system. Therefore, the pores in the structures were constructed by the aggregation of the polymer chains. The homogeneous cross-linking structures and high degree of cross-linking densities could be obtained in these polymers structures due to the small volumes and the less steric hindrance as well as the high reactivity of small molecules in presence of the catalyst. S_{BET} and the cross-linking densities of these polymers increased with the increasing amount of the cross-linking agents. However, in this report, bulky OVS was used as a crosslinker in the polymerization system. Rigid cage and multifunctionality make OVS quite different from small

molecule cross-linkers, such as divinylbenzene, monochlorodimethyl ether and dimethyl formal.^[47,48] Eight vinyl groups in one cage make it act as a concentrative crosslinker in the Friedel-Crafts reaction.^[39] The rigid cage makes it a potential nanobuilding block to form porous materials via the stacking of POSS cages.

Both OVS and PS could act as the host building blocks to construct porous materials in this study. It is therefore interesting to study the effect of the host-guest exchange of the two building blocks on the porosities of the resulting porous polymer networks by changing the ratio of PS and OVS. When OVS loading was lower than 9.1 wt % in this study, the resulting hybrid polystyrenes, *i.e.* HCP-1 and HP-2, were slightly crosslinked and dissolved in most common solvents, for example, THF, chloroform etc.. The resulting hybrid polystyrenes could not stack to form pores and exhibited no porosity by the BET measurements due to the lower crosslinking density.

When OVS loading was 9.1 wt % (*i.e.* HCP-3), a highly crosslinking network was formed, which favoured formation of pores and the resulting hybrid polystyrene did not dissolve in the common solvents and exhibited a maximum S_{BET} of $767 \text{ m}^2 \text{ g}^{-1}$. The pores in the networks were assigned to the aggregation of the polystyrene chains, in which OVS acted as a concentrative linker. Thereby, the local cross-linking density was higher, which resulted in high apparent specific surface. Meanwhile, the cross-linking density was inhomogeneous because of the relatively lower loading of the OVS. Consequently, the broader PSD was obtained. The structure of fragment A might be predominant in the resulting hybrid network when PS acted as the host building block (Scheme 1).

With further increasing OVS loading, on the one hand, most of vinyl groups might crosslink polystyrene, which generated more crosslinking points, the cross-linking density and the crosslinking homogeneity increased. The results lead to higher specific surface area and narrower PSD. Nonetheless, the number of the unreacted vinyl groups increased because of the steric effect of OVS, which had been confirmed by the FT-IR spectra. This resulted in the high free volumes of the networks, which decrease the S_{BET} of the hybrid polymers.^[44] In addition, the framework interpenetration^[45] might form due to the average crosslinking density between OVS and PS and resulted in the pore-filling in the networks, which decreased the apparent specific area of the networks. As a comprehensive result of these factors on porosity, S_{BET} decreased for HCP-4, HCP-5, HCP-6 and HCP-7 till no porosities.

When OVS loading was higher than 44.4 wt %, the obtained hybrid networks exhibited higher porosity again, for example, HCP-8 and HCP-9. For these hybrid materials, OVS acted as the host and these porosities arose from the stack of POSS cages in which, polystyrene act as a concentrative crosslinker. The structure of fragment B might dominate in the resulting hybrid crosslinking networks when OVS acted as the host (Scheme 1).

To evaluate the thermal stability of hypercrosslinking polymers, TGA was performed under N_2 at 10 min^{-1} from room temperature to $800 \text{ }^\circ\text{C}$. The results were shown in the Figure 5. Consistent with the previous reports,^[38,49] the initial decomposition temperatures of OVS and PS were about 250 and $370 \text{ }^\circ\text{C}$, respectively. Compared with pure PS, the decomposition temperatures of HCP-3 to HCP-9 were relatively similar and close to the pure PS. However, the residues of HCP-3 to HCP-9 at the $800 \text{ }^\circ\text{C}$ increased with the increase of OVS loading.

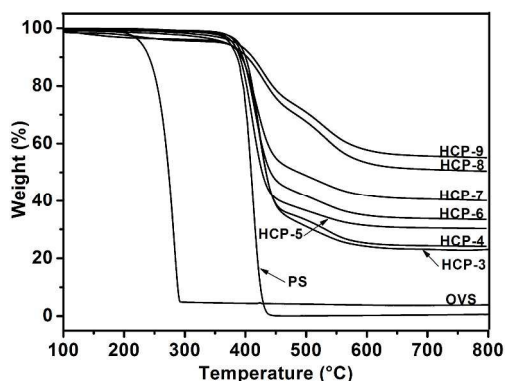


Figure 5. TGA curves of OVS, PS and HCP-3 to HCP-9

As expected, these hybrid polymers were amorphous and exhibited no long-range crystallographic order as revealed by powder X-ray diffraction (PXRD) (Figure 6). This result was similar to other nanoporous hybrid POSS-based materials. The HCP-3 to HCP-9 exhibited broad diffraction peaks at 2θ of $\sim 22^\circ$, which was typically observed in amorphous silica nanocomposites and associated with the Si–O–Si linkages.^[37] The particle size and internal morphologies of the polymers were characterized by the FE-SEM. In view of the similarity of the morphologies for these HPPs, HCP-3 was selected as a representative sample. The others images were displayed in the the supporting information (Figure S7 to S19). As shown in Figure 7 (a), the structure consisted of interlinking irregular shapes with nanostructure appearance and a wide range of diameters from 100 nm to tens of micrometers. All the samples were constructed by great amount of irregular particles with a wide range of size distribution ranging from 100 nm to several tens of micrometers. In order to further characterize the texture and ordering of these materials, high-resolution transmission electron microscopy (HR-TEM) was performed. The HCP-3 image (Figure 7 (b)) revealed that the polymer exhibited the features of amorphous porous materials without long-range ordering. The samples were stable under the electron beam.

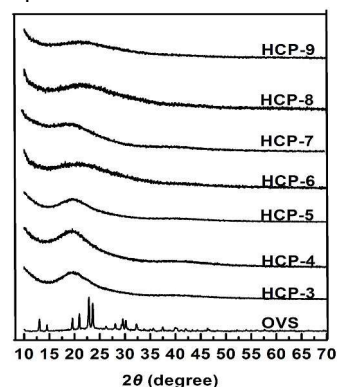


Figure 6. The XRD patterns of OVS and HCP-3 to HCP-9.

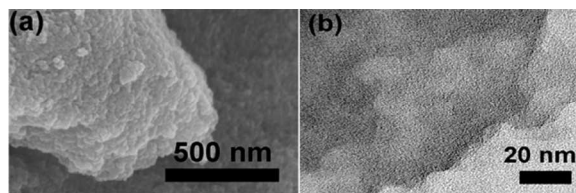


Figure 7. (a) SEM image of HPP-3 and (b) HRTEM image of HPP-3.

Gas storage is one of the important and promising applications of porous materials.^[50] In order to evaluate the gas storage performances of the obtained hybrid hypercrosslinking polymers, H₂ and CO₂ sorption experiments at 77 and 298 K were performed. Compared with the HCP-4, HCP-8 and HCP-9, HCP-3 possessed the highest surface area and pore volume. It was selected as an example to evaluate the H₂ and CO₂ sorption properties. The H₂ storage capacity for HCP-3 was 3.01 mmol g⁻¹ (0.60 wt%) at 1.01 bar, 77 K (Figure 8 (a)). The CO₂ uptake for HCP-3 was 1.12 mmol g⁻¹ (4.93 wt%) at 1.01 bar, 298 K (Figure 8 (b)). The adsorption capacities were comparable to those of other porous polymers with similar surface areas. For example, Germain et al.^[14] reported that the Amberlite XAD16 with a S_{BET} of 770 m² g⁻¹ exhibited a H₂ storage uptake of 0.6 wt% at 77.3 K and 0.12MPa; the Amberlite XAD16 was constructed from styrene and divinylbenzene building blocks. Dawson et al.^[51] reported that the CMP-1 with a S_{BET} of 839 m² g⁻¹ exhibited a CO₂ storage uptake of 1.18 mmol g⁻¹ at 298 K and 1 bar; CMP-1 was constructed from 1,3,5-triethynylbenzene and 2,5-dibromobenzene via Sonogashira–Hagihara palladium catalyzed cross-coupling reaction. These values suggested that HPPs could be considered as promising candidates for H₂ and CO₂ storage.

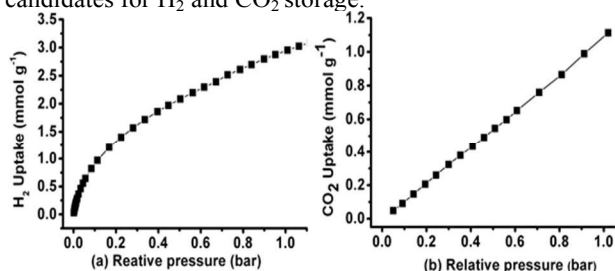


Figure 8. Gas sorption isotherms of HCP-3. (a) H₂ adsorption isotherm at 77 K. (b) CO₂ adsorption isotherm at 298 K.

Conclusions

In conclusion, octavinylsilsequioxane (OVS) reacted with commercial polystyrene to prepare hybrid porous hypercrosslinking polymers via the Friedel-Crafts alkylation through the ingenious design. The porosity can be fine-tuned by changing the ratio of PS to OVS. The resulting polymers HCP-1 to HCP-9 with the apparent Brunauer–Emmett–Teller surface areas (S_{BET}) were in a range of 2.6 to 767 m² g⁻¹, with total pore volumes in the range of 0.36 to 0.90 cm³ g⁻¹. The gas sorption applications revealed that HCP-3 possessed H₂ uptake of 3.01 mmol g⁻¹ (0.60 wt%) at 77 K and 1.01 bar and CO₂ uptake of 1.12 mmol g⁻¹ (4.93 wt%) at 298 K and 1.01 bar, which demonstrated that these materials had the potential to be applied in gas storage of H₂ and CO₂.

Acknowledgements

This research was supported by the National Natural Science Foundation of China (21274081).

Notes and references

^a Key Laboratory of Special Functional Aggregated Materials, Ministry of Education, School of Chemistry and Chemical Engineering Shandong University Jinan 250100, P. R. China Fax: (+86) 531 88564464 E-mail: liuhongzhi@sdu.edu.cn

^b Key Laboratory of Fine Chemicals in Universities of Shandong

Shandong Provincial Key Laboratory of Fine Chemicals, Qilu University of Technology, Jinan 250353, P. R. China

^c Key Laboratory of Specially Functional Polymeric Materials and Related Technology, Ministry of Education, East China University of Science and Technology, Shanghai, 200237.

We dedicate this paper to Prof. Hongzhi Liu's mother, who is dearly missed by all members of the family

†Electronic Supplementary Information (ESI) available: [The elemental analysis results of HCP-1 to HCP-9; FT-IR spectra of HCP-1, HCP-2, HCP-5 to HCP-7; FE-SEM images of HCP-3 to HCP-9 with different magnifications and areas.]. See DOI: 10.1039/b000000x

- [1] N. B. McKeown and P. M. Budd, *Chem. Soc. Rev.*, 2006, **35**, 675.
- [2] H. W. Oviatt, K. J. Shea, S. Kalluri, Y. Shi and W. H. Steier, *Chem. Mater.*, 1995, **7**, 493.
- [3] G.-H. Hsuie, R.-H. Lee, and R.-J. Jeng, *Chem. Mater.*, 1997, **9**, 883.
- [4] X. Du, Y. Sun, B. Tan, Q. Teng, X. Yao, C. Su and W. Wang, *Chem. Commun.*, 2010, **46**, 970.
- [5] D. Dang, P. Wu, C. He, Z. Xie and C. Duan, *J. Am. Chem. Soc.*, 2010, **132**, 14321.
- [6] D. Wu, F. Xu, B. Sun, R. Fu, H. He, and K. Matyjaszewski, *Chem. Rev.*, 2012, **112**, 3959.
- [7] S. Stankovich, D. Dikin, G. Dommett, K. Kohlhaas, E. Zimney, E. Stach, R. Piner, S. Nguyen and R. Ruoff, *Nature*, 2006, **442**, 282.
- [8] V. A. Davankov and M. P. Tsyurupa, *React. Polym.*, 1990, **13**, 27.
- [9] V. V. Podlesnyuk, J. Hradil and E. Králová, *React. Funct. Polym.*, 1999, **42**, 181.
- [10] V. V. Azanova and J. Hradil, *React. Funct. Polym.*, 1999, **41**, 163.
- [11] N. A. Penner and P. N. Nesterenko, *J. Chromatogr. A*, 2000, **884**, 41.
- [12] M. G. Kiseleva, L. V. Radchenko and P. N. Nesterenko, *J. Chromatogr. A*, 2001, **920**, 79.
- [13] J. Y. Lee, C. D. Wood, D. Bradshaw, M. J. Rosseinsky and A. I. Cooper, *Chem. Commun.*, 2006, 2670.
- [14] J. Germain, J. Hradil, J. M. J. Fréchet and F. Svec, *Chem. Mater.*, 2006, **18**, 4430.
- [15] M. Kaliva, G. S. Armatas and M. Vamvakaki, *Langmuir*, 2012, **28**, 2690.
- [16] R. Füllner, H. Schäfer and A. Seubert, *Anal. Bioanal. Chem.*, 2002, **372**, 705.
- [17] K. J. Balkus, Jr., A. Kortz and R. S. Drago, *Inorg. Chem.*, 1988, **27**, 2955.
- [18] J. Xu, G. Chen, n R. Ya, D. Wang, M. Zhang, W. Zhang and P. Sun, *Macromolecules*, 2011, **44**, 3730.
- [19] S. N. Sidorov, L. M. Bronstein, V. A. Davankov, M. P. Tsyurupa, S. P. Solodovnikov, P. M. Valetsky, E. A. Wilder and R. J. Spontak, *Chem. Mater.*, 1999, **11**, 3210.
- [20] J. Choi, S. G. Kim, and R. M. Laine, *Macromolecules*, 2004, **37**, 99.
- [21] Q. Yao, L. Chen, W. Zhang, S. Liufu and X. Chen, *ACS Nano*, 2010, **4**, 2445.
- [22] H. Zou, S. Wu, and J. Shen, *Chem. Rev.*, 2008, **108**, 3893.
- [23] H. Hu, W. Yuan, H. Zhao and G. L. Baker, *J. Polym. Sci. Part A: Polym. Chem.*, 2014, **52**, 121.
- [24] Z. Jia, W. Yuan, H. Zhao, H. Hua and G. L. Baker, *RSC Adv.*, 2014, **4**, 41087.
- [25] W. Yuan, H. Zhao, H. Hu, S. Wang and G. L. Baker, *ACS Appl. Mater. Interf.*, 2013, **5**, 4155.
- [26] D. B. Cordes, P. D. Lickiss and F. Rataboul, *Chem. Rev.*, 2010, **110**, 2081.
- [27] L. Li, H. Liu, *RSC Advances*, 2014, **4**, 46710.
- [28] I. Blanco, L. Abate, F. A. Bottino and P. Bottino, *Polym. Degrad. Stab.*, 2012, **97**, 849.
- [29] J. Wu, T. S. Haddad, G. M. Kim and P. T. Mather, *Macromolecules*, 2007, **40**, 544.
- [30] A. Romo-Uribe, P. T. Mather, T. S. Haddad, J. D. Lichtenhan, *J. Polym. Sci. Part B: Polym. Phys.*, 1998, **36**, 1857.
- [31] X. Song, H. Geng and Q. Li, *Polymer*, 2006, **47**, 3049.
- [32] N. Hao, B. Mollhning, and A. Scholnhals, *Macromolecules*, 2007, **40**, 9672.
- [33] X. Zou, H. Rena and G. Zhu, *Chem. Commun.*, 2013, **49**, 3925.
- [34] X. Feng, X. Ding and D. Jiang, *Chem. Soc. Rev.*, 2012, **41**, 6010.

Journal Name

- [35] D. Wang, W. Yang, S. Feng and H. Liu, *Polym. Chem.*, 2014, **5**, 3634.
- [36] C. X. Zhang, F. Babonneau, C. Bonhomme, R. M. Laine, C. L. Soles, H. A. Hristov, A. F. Yee, *J. Am. Chem. Soc.*, 1998, **120**, 8380.
- [37] W. Chaikittisilp, M. Kubo, T. Moteki, A. Sugawara-Narutaki, A. Shimojima and T. Okubo, *J. Am. Chem. Soc.*, 2011, **133**, 13832.
- [38] Y. Wu, D. Wang, L. Li, W. Yang, S. Feng and H. Liu, *J. Mater. Chem. A*, 2014, **2**, 2160.
- [39] W. Yang, D. Wang, L. Li, and H. Liu, *Eur. J. Inorg. Chem.*, **2014**, 2976.
- [40] D. Chen, S. Yi, W. Wu, Y. Zhong, J. Liao, C. Huang and W. Shi, *Polymer*, 2010, **51**, 3867.
- [41] F. Alves, P. Scholder and I. Nischang, *ACS Appl. Mater. Interfaces*, 2013, **5**, 2517.
- [42] Y. Peng, T. Ben, J. Xu, M. Xue and S. Qiu, *Dalton Trans.*, 2011, **40**, 2720.
- [43] W. Chaikittisilp, A. Sugawara, A. Shimojima and T. Okubo, *Chem. Eur. J.*, 2010, **16**, 6006.
- [44] D. Wang, W. Yang, L. Li, X. Zhao, S. Feng and H. Liu, *J. Mater. Chem. A*, 2013, **1**, 13549.
- [45] Y. Wada, K. Iyoki, A. Sugawara-Narutaki, T. Okubo and A. Shimojima, *Chem. Eur. J.*, 2013, **19**, 1700.
- [46] M. P. Tsyurupa and V. A. Davankov, *React. & Funct. Polym.*, 2006, **66**, 768.
- [47] F. Maya and F. Svec, *Polymer*, 2014, **55**, 340.
- [48] B. Li, X. Huang, L. Liang and B. Tan, *J. Mater. Chem.*, 2010, **20**, 7444.
- [49] Y. Li and J. Ma, *Polym. Degrad. Stab.*, 2001, **73**, 163.
- [50] F. Vilela, K. Zhang and M. Antonietti, *Energy Environ. Sci.*, 2012, **5**, 7819.
- [51] R. Dawson, D. J. Adams and A. I. Cooper, *Chem. Sci.*, 2011, **2**, 1173.